The American Journal of Pathology, Vol. 181, No. 1, July 2012

http://dx.doi.org/10.1016/j.ajpath.2012.03.042

Immunopathology and Infectious Diseases

Role of SOCS2 in Modulating Heart Damage and Function in a Murine Model of Acute Chagas Disease

Lisia Esper,*† Danilo Roman-Campos,* Aline Lara,‡ Fatima Brant,* Luisa L. Castro,* Andreia Barroso,* Ronan Ricardo S. Araujo,* Leda Q. Vieira,*§ Shankar Mukherjee,¶ Eneas Ricardo M. Gomes,‡ Nazareth N. Rocha,‖ Isalira P.R. Ramos,‖ Michael P. Lisanti,** Camila F. Campos,†† Rosa M.E. Arantes,†† Silvia Guatimosim,‡ Louis M. Weiss,¶ Jader Santos Cruz,* Herbert B. Tanowitz,¶ Mauro M. Teixeira,*† and Fabiana S. Machado*†

From the Departments of Biochemistry and Immunology, Physiology and Biophysics,‡ and Pathology,†† Institute of Biological Science, and the Program in Health Sciences, Infectious Diseases and Tropical Medicine,† Medical School, Federal University of Minas Gerais, Belo Horizonte, Brazil; the Post-Graduate Program in Biological Sciences,§ Federal University of Ouro Preto, Ouro Preto, Brazil; the Departments of Pathology and Medicine,¶ Albert Einstein College of Medicine, Bronx, New York; the Department of Physiology and Pharmacology,‖ Fluminense Federal University, Niteroi, Brazil; and the Department of Stem Cell Biology and Regenerative Medicine,** Kimmel Cancer Center, Thomas Jefferson University, Philadelphia, Pennsylvania*

Infection with *Trypanosoma cruzi* induces inflammation, which limits parasite proliferation but may result in chagasic heart disease. Suppressor of cytokine signaling 2 (SOCS2) is a regulator of immune responses and may therefore participate in the pathogenesis of *T. cruzi* infection. SOCS2 is expressed during *T. cruzi* infection, and its expression is partially reduced in infected 5-lipoxygenase–deficient [knockout (KO)] mice. In SOCS2 KO mice, there was a reduction in both parasitemia and the expression of interferon-γ (IFN-γ), tumor necrosis factor-α (TNF-α), IL-6, IL-10, SOCS1, and SOCS3 in the spleen. Expression of IFN-γ, TNF-α, SOCS1, and SOCS3 was also reduced in the hearts of infected SOCS2 KO mice. There was an increase in the generation and expansion of T regulatory (Treg) cells and a decrease in the number of memory cells in *T. cruzi*–infected SOCS2 KO mice. Levels of lipoxinA_4 (LXA_4) increased in these mice. Echocardiography studies demonstrated an impairment of cardiac function in *T. cruzi*–infected SOCS2 KO mice. There were also changes in calcium handling and in action potential waveforms, and reduced outward potassium currents in isolated cardiac myocytes. Our data suggest that reductions of inflammation and parasitemia in infected SOCS2-deficient mice may be secondary to the increases in Treg cells and LXA_4 levels. This occurs at the cost of greater infection-associated heart dysfunction, highlighting the relevance of balanced inflammatory and immune responses in preventing severe *T. cruzi*–induced disease. ***(Am J Pathol 2012, 181:130–140; http://dx.doi.org/10.1016/j.ajpath.2012.03.042)***

Chagas disease is caused by infection with the protozoan parasite *Trypanosoma cruzi.* This infection results in acute myocarditis and chronic cardiomyopathy. Chagasic cardiomyopathy is the result of intense multifocal progressive inflammation of the myocardium[1] and damage to the vascular endothelium[2–4] resulting in vasospasm and reduction in blood flow.[5] Chronic chagasic heart disease may manifest insidiously as congestive heart failure or abruptly with arrhythmias, conduction abnormalities, and/or thromboembolic events. Dilated congestive cardiomyopathy is an important manifestation

Supported by PRPq-UFMG (F.S.M.), CNPq (576200/2008-5, 473670/2008-9; to F.S.M.), FAPEMIG (PPM-00378-09; to F.S.M.), NIH grant AI-076248 (H.B.T.), and a Scientist Development Grant of the American Heart Association #0735252N (S.M.).

Accepted for publication March 7, 2012.

A guest editor acted as editor-in-chief for this manuscript. No person at Thomas Jefferson University or Albert Einstein College of Medicine was involved in the peer review process or final disposition for this article.

Address reprint requests to Fabiana Simao Machado, Ph.D., Institute of Biological Sciences (UFMG-ICB), Department of Biochemistry and Immunology, Federal University of Minas Gerais, Bloco O4, 190 Av. Antônio Carlos, 6627 Pampulha, 31270-901 Belo Horizonte, MG, Brazil. E-mail: machadofs@icb.ufmg.br.

and usually occurs years or even decades after the initial infection.[6] Pathological examination of the heart reveals chronic inflammation and fibrosis. Electrocardiography, echocardiography, and cardiac magnetic resonance imaging are useful in assessing the severity of disease in experimental animals and humans.[6]

Protective immunity against *T. cruzi* is characterized by a T helper type 1 (T_{H1})-type response where the cytokines interferon-γ (IFN-γ), tumor necrosis factor-α (TNF-α), and IL-12 contribute to the control of parasite replication.[7–9] Early in infection, several *T. cruzi*–derived molecules, including glycosylphosphatidylinositol mucins and parasite DNA[10,11] stimulate the synthesis of IL-12 and TNF-α by macrophages.[12] Once secreted *in vivo*, IL-12 induces natural killer (NK) cells to synthesize IFN-γ, which in turn induces increased levels of IL-12 that cycles back to enhance IFN-γ production by NK cells. IFN-γ production is also amplified by IFN-γ–induced production of macrophage TNF-α and IL-1β by a positive feedback loop. Importantly, these cytokines drive the generation of type 1 $CD4^+$ and $CD8^+$ T cells, which produce further IFN-γ, a key requirement for inducing and maintaining control of acute infection.[13] The down-regulatory cytokines IL-10 and transforming growth factor-β (TGF-β) are associated with susceptibility to infection[13,14] by inhibiting IFN-γ–mediated macrophage activation. Resistance to the initial infection is a result of a balance between proinflammatory IFN-γ and anti-inflammatory IL-10 production.[13] The immune response generated to *T. cruzi* is largely effective at controlling, but not eliminating, the infection, which is life-long unless treatment is provided.

Suppressor of cytokine signaling 2 (SOCS2) is known to have important actions in the regulation of various cytokine/growth hormone-mediated processes, including somatic growth, metabolism, and response to infection.[15,16] Among the SOCS family, SOCS2 may regulate the expression of other members, including SOCS1 and SOCS3,[15,17] effects that may eventually result in enhanced function of certain cytokines. Importantly, SOCS2 is known to regulate the cytokine-dependent Janus kinase (JAK)/signal transducers and activators of transcription (STAT) signaling pathway in cells of the innate and adaptive immune systems, modulating the production of several mediators, including TNF-α and IL-12,[15,16,18] and favoring T helper 2 (Th2) differentiation and production of Th2 cytokines.[18] SOCS2 is involved in the regulation of immune response in *T. gondii* infection.[16,19] Because SOCS2 plays a role in certain infections and has been shown to modulate cytokines that are crucial for the pathogenesis of *T. cruzi* infection, we conducted studies to evaluate the expression and potential role(s) of SOCS2 in the pathogenesis of *T. cruzi*–induced heart disease. We present evidence for a role for SOCS2 in the modulation of experimental *T. cruzi* infection and suggest how it may interfere with cardiac function. These data provide a new insight into the pathogenesis of chagasic heart disease as well as provide novel therapeutic targets to ameliorate disease progression.

Materials and Methods

Mice

Wild-type (WT) C57BL/6 mice were obtained from CEBIO [Centro de Bioterismo–Universidade Federal de Minas Gerais (UFMG)]. 5-Lipoxygenase (5-LO) KO (129-Alox5^{tm1Fun}/J; as described by Chen et al[20]) and SOCS2 KO (as described by Metcalf et al[21]) mice were kindly provided by Dr. Fernando Queiroz Cunha (University of Sao Paulo, Ribeirao Preto, Brazil) and Dr. Warren S. Alexander (the Walter and Eliza Hall Institute of Medical Research, Australia), respectively. 5-LO KO strain–matched WT mice were kindly provided by Dr. Vanessa Pinho da Silva (Federal University of Minas Gerais). All animal lineages were bred and maintained under pathogen-free conditions at the Institute of Biological Sciences–UFMG animal facility. All animal experiments were approved by the local animal ethics committee.

Parasites and Experimental Infection

The Y strain of *T. cruzi* was maintained in C57BL/6 mice. Seven- to 8-week-old WT and KO mice were infected intraperitoneally with 1×10^3 trypomastigotes, and parasitemia determined daily in 5 μL of blood collected from a tail vein.[22] For *in vitro* infection, trypomastigotes were grown and purified from a monkey kidney epithelial cell line (LLC-MK2).

Macrophage Culture, Evaluation of NO_2^- Production, and Microbicidal Activity

WT and SOCS2 KO inflammatory macrophages were harvested from peritoneal cavities 3 days after injection of 1 mL of 3% sodium thioglycollate. The cells were washed and cultured (1×10^6 cells/mL) in RPMI 1640 (Sigma-Aldrich, St. Louis, MO), supplemented with 5% fetal bovine serum, 50 μmol/L 2-mercaptoethanol, 2 mmol/L L-glutamine, and penicillin/streptomycin (all from GIBCO, Grand Island, NY). The adherent cells were obtained after 2 to 4 hours of incubation of single-cell suspensions in tissue culture plates at 37°C in 5% CO_2. Nonadherent cells were removed, and trypomastigote forms were added at a 5:1 parasite-to-cell (macrophage) ratio for 3 hours, after which the extracellular parasites were removed, and the cells were incubated at 37°C in 5% CO_2 in the presence or absence of 100 ng/mL of recombinant murine IFN-γ (GIBCO). The supernatants were harvested 24, 48, and 72 hours post infection and assayed for nitrite concentration by mixing 0.1 mL of culture supernatant with 0.1 mL of Griess reagent. Absorbance at 540 nm was read 10 minutes later, and NO_2^- concentration was determined. Macrophages were infected, the extracellular parasites were removed, and the cells were incubated with or without IFN-γ as described above. Parasite growth was evaluated by daily counting of the trypomastigotes in the supernatant of infected macrophages on days 3 to 7 post infection. The intracellular amastigote growth rate was evaluated in macrophages plated (5×10^5 cell/mL) onto chamber slides (Nalge Nunc, Naperville, IL), as described.[8,22]

Isolation of Left Ventricular Myocytes

Left ventricular cardiac myocytes from age-matched mice were enzymatically isolated as previously described, with minor modifications.[23] Hearts were quickly removed, mounted, and then perfused using a customized Langendorff apparatus for 5 minutes with nominally Ca^{2+}-free solution containing 130 mmol/L NaCl, 5.4 mmol/L KCl, 0.5 mmol/L $MgCl_2$, 0.33 mmol/L NaH_2PO_4, 3 mmol/L pyruvate, 22 mmol/L glucose, and 25 mmol/L HEPES (pH 7.4). Hearts were then perfused for 10 to 15 minutes at 37°C with a solution containing 1 mg/mL type II collagenase (Worthington Biochemical Corporation, Lakewood, NJ). The digested heart was removed from the cannula, and the left and/or right ventricular free wall was separated, gently agitated, centrifuged (180 × *g*, 10 seconds at room temperature) and stored in Dulbecco's modified Eagle's medium (Sigma-Aldrich). The isolated cardiac myocytes were stored at room temperature and used within 4 to 6 hours of isolation. Only calcium-tolerant, quiescent, rod-shaped myocytes showing clear cross striations were studied.

Whole-Cell Ruptured, Patch Clamp Technique

Whole-cell voltage and current-clamp recordings were obtained using an EPC-9.2 patch clamp amplifier (HEKA Electronics, Lambrecht/Pfalz, Germany).[24] On attaining the whole-cell configuration, the cells were equilibrated for 3 to 5 minutes in the pipette solution. The experiments were carried out at room temperature (24°C to 27°C). The recording electrodes had resistances of 0.5 to 1.5 MΩ. Current recordings were low-pass filtered (2.9 kHz) and digitized at 10 kHz before being stored on a computer. Myocytes showing series resistance (Rs) larger than 7 MΩ were not used in the analysis. Rs compensation was used at 40% to 70%. We used Tyrode's as a bath solution of 140 mmol/L NaCl, 5.4 mmol/L KCl, 1 mmol/L $MgCl_2$, 1.8 mmol/L $CaCl_2$, 10 mmol/L glucose, 10 mmol/L HEPES (pH 7.4). For measurements of $I_{Ca,L}$, recording pipettes were filled with internal solution containing 120 mmol/L CsCl, 20 mmol/L TEACl, 5 mmol/L NaCl, 10 mmol/L HEPES, 5 mmol/L EGTA, pH set to 7.2 with CsOH. $I_{Ca,L}$ was recorded in the presence of 1.8 mmol/L extracellular Ca^{2+}. Membrane potential was first stepped from a holding potential of −80 mV to −40 mV for 50 ms (to inactivate Na^+ channels), and then stepped to different membrane voltages between −40 to 50 mV (300-ms duration). To measure action potentials (AP) and outward potassium current (I_{to}), pipette solution contained 130 mmol/L potassium aspartate, 20 mmol/L KCl, 10 mmol/L HEPES, 2 mmol/L $MgCl_2$, 5 mmol/L NaCl, 5 mmol/L EGTA, pH set to 7.2 with KOH. With regular Tyrode's as a bath solution, we recorded 30 to 50 AP per cell (at 1 Hz), until a stable recording condition was achieved, and we used the last recorded AP to perform the complete analysis. I_{to} was elicited by depolarization steps from −40 to 70 mV (3-seconds duration) from a holding potential of −80 mV at a stimulation frequency of 0.066 Hz. We used a 50-ms pre-pulse to −40 mV from −80 mV to inactivate I_{Na} but still be able to record I_{to}.[24]

Current-density relationships were fitted using the following equation:

$$I_{(V)} = G_{max} * \frac{(V_m - E_i)}{1 + \exp(V_m - V_{0.5}) / S} \quad (1)$$

where G_{max} is the maximal conductance; V_m is the test membrane potential; E_i, electrochemical equilibrium potential for ion *i*; $V_{0.5}$ is the membrane potential where 50% of the channels are activated; and *S* is the slope factor.[23,24]

Echocardiography

Echocardiography (Visual Sonics, Toronto, ON, Canada) was performed on mice anesthetized with 1.5% isoflurane. Heart morphology was assessed using M-mode configuration. Cardiac output and ejection fraction were obtained from the B-mode according to Simpson's method. All parameters were evaluated following protocols of the American Society of Echocardiography.[25]

Transient Ca^{2+} Recordings

Adult ventricular myocytes were isolated as described above, and intracellular Ca^{2+} ($Ca^{2+}{}_i$) imaging experiments were performed as described[26] with cardiac myocytes loaded with Fluo-4 AM (10 μmol/L; Invitrogen, Eugene, OR) for 25 minutes. Cells were electrically stimulated at 1 Hz to produce steady-state conditions. The confocal line-scan imaging was performed with a Zeiss LSM 510META confocal microscope (Carl Zeiss, Oberkochen, Germany) (Centro de Microscopia Eletronica, UFMG). Digital image processing was performed by using custom-devised routines created with the IDL programming language (Research Systems, Boulder, CO). The Ca^{2+} level was reported as F/F_0, where F_0 is the resting Ca^{2+} fluorescence.

LipoxinA_4 and Cytokine Determinations

The concentration of LipoxinA_4(LXA_4) was measured using commercially available antibodies and according to the procedures supplied by the manufacturer (Neogen, Lexington, KY). IL-12 p40 and IFN-γ levels were measured using commercial ELISA kits (BD Biosciences/Pharmingen, San Jose, CA, and R&D Systems, Minneapolis, MN, respectively). For *in vivo* experiments, a minimum of five mice were infected as described above, and on different days post infection were bled for assessment of cytokine levels in the serum.

Total RNA Extraction and cDNA Preparation by Reverse Transcription

Total RNA was isolated from mouse cardiac and splenic tissue, homogenized in 1 mL of Brazol reagent (LGC Biotecnologia, Cotia, Brazil) according to the manufacturer's instructions, followed by the addition of 0.2 mL of chloroform (Sigma-Aldrich). Purified RNA (2 μg) was used to synthesize cDNA using Superscript II (GIBCO).

Parasite Load, Cytokines, and SOCS mRNA Detection

The expression of mRNA for cytokines (IL-6, IL-10, IL-12, TNF-α, and IFN-γ), SOCS1, SOCS2, SOCS3, and β-actin was analyzed by RT-PCR, with GoTaqGreen Master Mix (Promega, Madison, WI) in a PTC-100 thermal cycler (MJ Research, Alameda, CA). The reaction conditions were 34 cycles of 1 minute at 94°C, 1 minute at 60°C, and 1 minute at 72°C, with a final extension step of 2 minutes at 72°C. The parasite load was detected using a *T. cruzi*–specific primer (rDNA 24S α). Reaction conditions were 30 cycles of 1 minute at 94°C, 1 minute at 60°C, and 1 minute at 72°C, with a final extension step of 10 minutes at 72°C. PCR products were separated by agarose gel electrophoresis and stained with ethidium bromide. The primer sequences and PCR products for cytokines and β-actin have been described before.[16] The primer sequences for *T. cruzi* load were (forward: 5′-AAGGTGCGTCGACAGTGTGG-3′ and reverse: 5′-TTTTCAGAATGGCCGAACAGT-3′), 125 bp.

Spleen Cell Cultures

Suspensions of splenocytes from uninfected and chronically *T. cruzi*–infected mice (6 months post infection) were washed in Hanks' balanced salt solution and treated with lysis buffer [nine parts 0.16 mmol/L ammonium chloride and one part 0.17 mmol/L Tris-HCl (pH 7.5)] for 4 minutes. The erythrocyte-free cells were then washed three times in Hanks' balanced salt solution and adjusted to cells per mL of RPMI 1640 (Sigma-Aldrich) supplemented with 10% fetal calf serum (Cultilab, Campinas, Brazil), 2-mercaptoethanol (Invitrogen), L-glutamine (GIBCO), and penicillin/streptomycin (all from GIBCO). The cell suspension was cultured in 24-well tissue-culture plates (1 mL/well; Nalge Nunc) for 48 hours at 37°C, 5% CO_2 atmosphere, either in the presence or absence of trypomastigotes (five parasites per cell) or *T. cruzi* antigen (10 μg/mL). The supernatants were harvested, and IFN-γ levels were measured using commercial enzyme-linked immunosorbent assay (ELISA) kits (R&D Systems).

Flow Cytometry Analysis

Splenocytes were purified from the *T. cruzi*–infected mice [0, 8, 15, 29, or 180 days post infection (dpi)] as described above. Splenocytes purified from 0 and 15 dpi were plated and incubated with brefeldin A (1 μg/mL) (Invitrogen). Four hours post treatment, the cells were fixed and stained with labeled antibodies against IFN-γ (fluorescein isothiocyanate), CD4 (phycoerythrin), or CD8 (peridinin chlorophyll protein complex) (BD Biosciences/Pharmingen). Cells harvested from spleen and thymus 0, 8, 15, and 29 days post infection were directly stained with the combination of CD4 (peridinin chlorophyll protein complex), CD25 (phycoerythrin), and FOXP3 (fluorescein isothiocyanate) specific antibodies. Viable cells were analyzed by flow cytometry using FlowJo software version 8.7 (Tree Star, Ashland, OR).

Heart Histopathology, Morphometric Analysis, and Parasitism

To compare the effects of SOCS2 expression on the influx of inflammatory cells in the heart, we analyzed the pattern and intensity of myocarditis by morphometry. For this experiment, the hearts from three mice from each group were removed at 15 days post infection and cut transversally. Each heart was washed in phosphate-buffered saline and fixed in 4% phosphate-buffered formaldehyde. After 24 hours of fixation, the tissues were paraffin-embedded, and three 5-μm-thick, semiconsecutive sections were stained by H&E for inflammation assessment or by Trichrome to evaluate fibrosis. Inflammation and fibrosis were assessed both in the atrial and ventricular free walls and in the interventricular septum, in five fields from each H&E- or Trichrome-stained section randomly chosen at a $\times$20 objective magnification, analyzing a myocardial area of 1.5×10^6 μm^2 per field. Images were captured at a resolution of 1392 $\times$ 1040 pixels with a CoolSNAP-Pro cf color microcamera (Media Cybernetics, Bethesda, MD) and analyzed in Image-Pro Express, version 4.0 (Media Cybernetics) and KS300 software (Carl Zeiss, Jena, Germany). An automatic macro recorder assembler (an algorithm of the KS300 software) was elaborated for capture, image processing, and segmentation, definition of morphometry conditions and counts of all of the cells detected in each image. The nucleus from each cell presented in the analyzed fields were counted and expressed as cells per field. Fibrosis was assessed using the image segmentation function. All pixels with blue hues in the Trichrome sections were selected to build a binary image and subsequently to calculate the total area occupied by connective tissue per field (fibrosis area per field). Heart parasitism was qualitatively evaluated by counting the number of parasite nests in three semiconsecutive sections as visualized by light microscopy with an $\times$40 objective.

Statistical Analysis

The statistical significance of differences in mean values between experimental versus control or vehicle-treated samples was evaluated by Student's *t*-test, one-way analysis of variance, or two-way analysis of variance. Bonferroni corrections were used as needed for multiple comparisons. Differences were considered to be significant at $P < 0.05$.

Results

Expression of SOCS2 in Infected Mice Is Partially 5-LO Dependent

5-LO activation and eicosanoid production, mainly LXA_4, may be involved in the modulation of SOCS2 expression. SOCS2 expression was increased in the spleen and cardiac tissue of *T. cruzi*–infected WT mice (Figure 1, A and B). There was a partial reduction in the expression of SOCS2 in both organs of 5-LO KO mice, indicating that products of this enzyme contribute to SOCS2 expression.

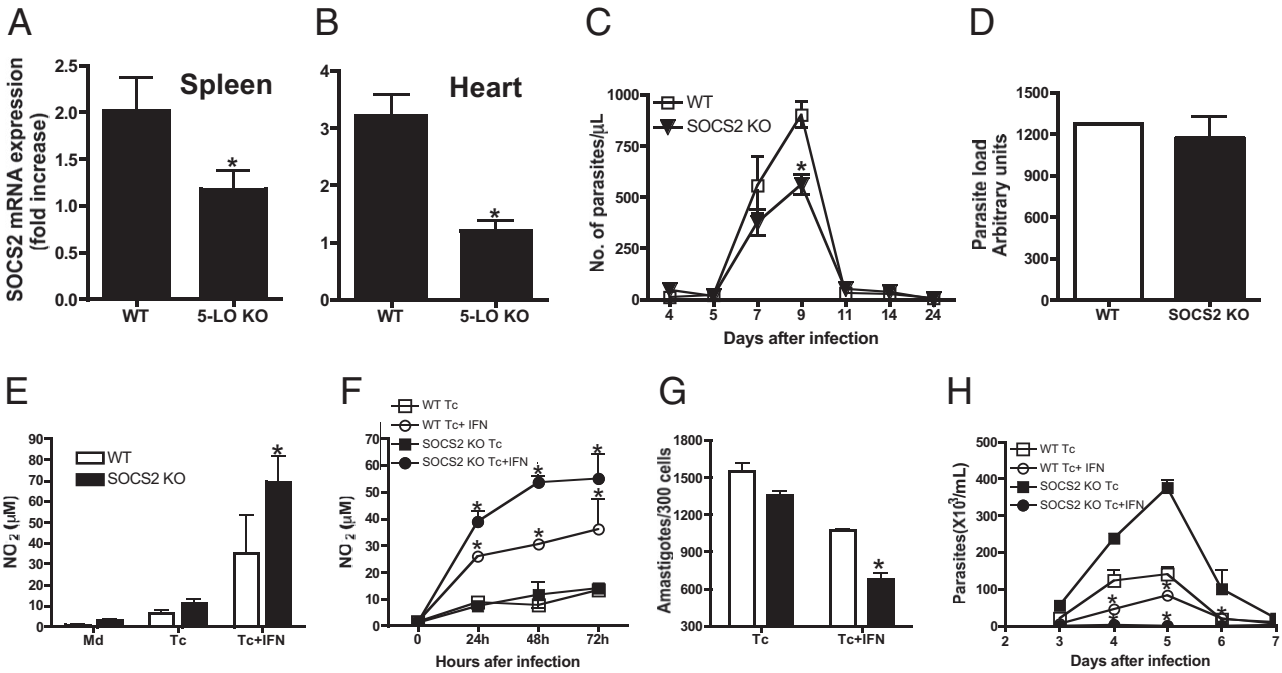

Figure 1. Parasitemia, tissue parasitism, and macrophage function of *T. cruzi*–infected SOCS2 KO mice. To determine the role of 5-LO in the expression of SOCS2, WT, SOCS2 KO, and 5-LO KO mice were infected intraperitoneally with 10^3 trypomastigotes of *T. cruzi* (Y strain), and the spleen and heart were examined 15 days post infection. WT and 5-LO KO mice were infected, and spleens (**A**) and hearts (**B**) were harvested and homogenized, mRNA extracted, and then RT-PCR performed using primers specific for the genes for SOCS2 and β-actin. Data were normalized to β-actin expression and to noninfected control mice. Note that there was a partial decrease in the expression of SOCS2 both in the heart and spleen of 5-LO KO mice. **C:** Parasitemia in WT and SOCS2 KO mice. Note the reduction in the SOCS2 KO mice. **D:** The parasite load was detected by PCR using a *T. cruzi*–specific prime (primer rDNA 24S α, TCr) in the heart. There were no differences in parasite load between WT and SOCS2 KO mice. Nitrite levels were assayed at (**E**) 48 hours and (**F**) as shown, in supernatants of *T. cruzi*–infected macrophages (Tc) and/or stimulated with IFN-γ (IFN). Uninfected macrophages cultured with medium (Md) alone were used as controls. WT and SOCS2 KO macrophages were infected (Tc) and treated with IFN-γ (Tc+IFN), cultured for (**G**) 48 hours, washed, fixed, and stained, and intracellular amastigotes were counted in 300 cells. **H:** The released trypomastigote forms were counted daily. **A–D:** Data are shown as the mean ± SD of the number of the parasites per microliter of blood from one of two independent experiments (eight mice per group). $^*P < 0.001$, for SOCS2 versus WT mice infected with *T. cruzi*. **E–G:** Each point represents mean ± SD of triplicate samples and is representative of three separate experiments. $^*P < 0.05$ versus values obtained in absence of parasites and/or cytokines.

SOCS2 Expression and Its Effects on Parasitemia, Tissue Parasitism, and Macrophage Function During T. cruzi *Infection in Mice*

Parasitemia was significantly reduced in SOCS2 KO mice compared with WT mice (Figure 1C). There was no significant difference in parasite load in the heart WT and SOCS2 KO mice (Figure 1D). Macrophages obtained from SOCS2 KO mice were hyperresponsive to IFN-γ stimulation, producing higher levels of NO (Figure 1, E and F) and increased parasite killing compared with WT macrophages (Figure 1, G and H). However, nonstimulated SOCS2 infected macrophages were more susceptible to infection than WT cells (Figure 1H).

Inflammatory Cytokine Responses, Expansion of T Regulatory and Memory Cells Are Controlled by a Regulatory Pathway Dependent on SOCS2 in Vivo

We evaluated the immune response to *T. cruzi* in SOCS2 KO mice. There was significantly decreased expression of IL-6, TNF-α, IL-12, IFN-γ, and IL-10 in the spleen (Figure 2A) and of TNF-α and IFN-γ in the heart (Figure 2B) of *T. cruzi*–infected SOCS2 KO mice when compared to those of infected WT mice. Infection of SOCS2 KO mice resulted in reduced expression of SOCS1 and SOCS3 in spleen and heart (Figure 2, A and B). Decreased systemic levels of IL-12 and IFN-γ were observed 9 days post infection in SOCS2 KO mice (Figure 3A). The number of T_{H1} IFN-γ–producing $CD4^+$ as well $CD8^+$ T cells was reduced in infected SOCS2 KO mice (Figure 3B).

To investigate the basis for these observations, we determined both LXA_4 production and the generation/expansion of Treg during *T. cruzi* infection. There was an increase in LXA_4 in the spleen (Figure 3C) and increased numbers of Treg cells in the thymus and spleen of *T. cruzi*–infected SOCS2 KO mice when compared with WT infected counterparts (Figure 3D). TGF-β levels were increased and IL-10 levels decreased in spleen of infected SOCS2 KO mice compared with WT mice (data not shown). Additionally, SOCS2 deficiency resulted in a reduction in the generation of memory T cells specific for *T. cruzi*. SOCS2-deficient lymphocytes harvested from chronically infected mice produced reduced levels of IFN-γ during recall responses *in vitro* when compared with WT infected mice (Figure 3E).

Myocardial Inflammation Is Reduced in SOCS2 KO Mice

The impact of SOCS2 deficiency on the development of infection-induced myocarditis was next examined. There

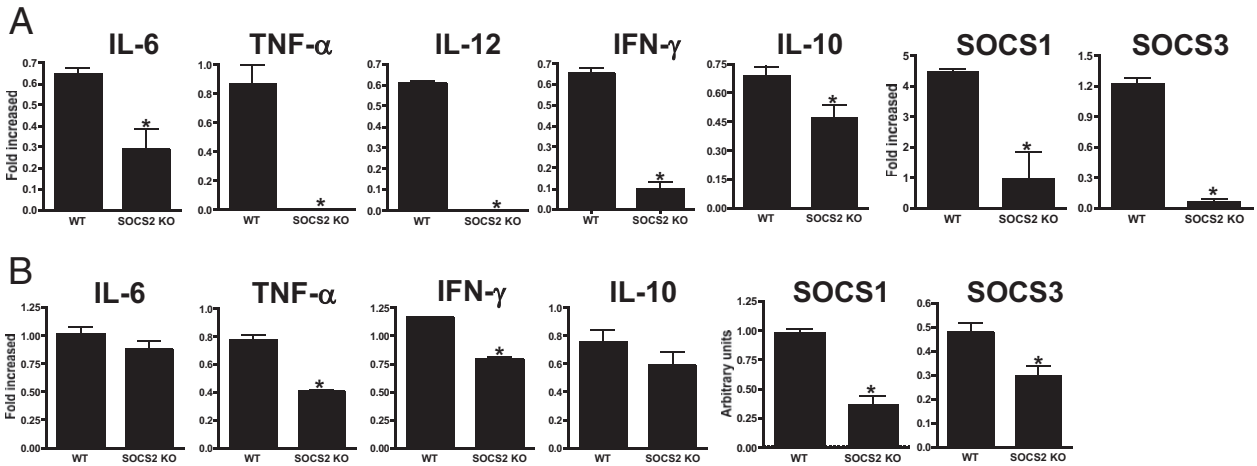

Figure 2. To determine whether there were changes in the expression of cytokines and SOCS1 and SOCS3 in the heart and spleen of infected SOCS2 KO mice. WT and SOCS2 KO mice were infected with 10^3 trypomastigotes Y (*T. cruzi*), and 15 days post infection, spleens (**A**) and hearts (**B**) were harvested, homogenized, mRNA extracted, and then RT-PCR performed using primers specific for the genes for IL-6, TNF-α, IL-12, IFN-γ, IL-10, SOCS1, and SOCS3. Data were normalized to β-actin expression and to control mice. Data are shown as the means ± SD and are representative of two independent experiments. $^*P < 0.05$ for SOCS2 versus WT mice infected with *T. cruzi*. Note the significant reduction in SOCS1 and SOCS3 expression and several proinflammatory cytokines.

was intense lymphocytic myocarditis and deposition of collagen in the myocardium of WT mice 15 days post infection (Figure 4). By contrast, there was only mild myocarditis and few nests of inflammatory cells in infected SOCS2 KO mice (Figure 4). However, no difference in the number of parasite nests was found between WT and SOCS2 KO mice (data not shown).

SOCS2 Expression Is Critical for Cardiac Myocyte/Cardiac Function During T. cruzi *Infection*

Declining cardiac function is a significant source of mortality in both experimental models and in patients suffering from Chagas disease. The effects of SOCS2 deficiency in the modulation of immune response and

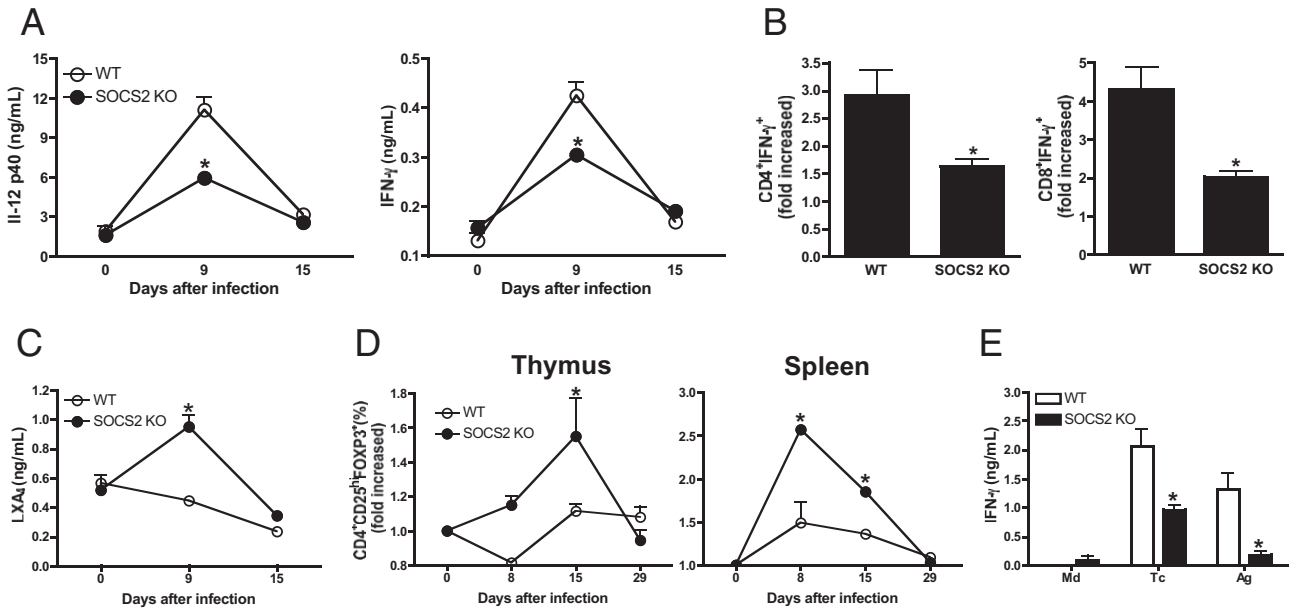

Figure 3. To determine whether there was a modulation of the inflammatory response, generation of effector, memory, and regulatory T cells in *T. cruzi*–infected SOCS2 KO mice 15 days post infection was assessed. **A:** The levels of IL-12 p40 and IFN-γ were observed in the serum of infected SOCS2 KO mice as compared to infected WT controls by ELISA. **B:** Splenocytes from WT and SOCS2 KO mice were incubated with brefeldin for 4 hours, followed by intracellular detection of IFN-γ in $CD4^+$ or $CD8^+$ T cells by flow cytometry. There was a reduction in IFN-γ in splenocytes from infected SOCS2 KO mice. **C:** The levels of LXA_4 were increased in the spleen of infected SOCS2 KO mice as compared to infected WT controls by ELISA. **D:** Similarly, at 0, 8, 15, and 29 days post infection, splenocytes and thymocytes were prepared for detection of $CD4^+CD25^+FOXP3^+$ cells by flow cytometry. There was an increase in $CD4^+CD25^{hi}FOXP3^+$ cells in the these cells obtained from infected SOCS2 KO mice. **E:** Splenocytes from WT and SOCS2 KO mice chronically infected with *T. cruzi* (6 months) were incubated with medium only (Md), *T. cruzi* trypomastigotes (Tc), or *T. cruzi* antigen (Ag) *in vitro* for 48 hours. Incubation was followed by the detection of IFN-γ in the supernatant by ELISA. There was a reduction in IFN-γ in the supernatant from infected SOCS2 KO mice. Data are shown as the means ± SD and are representative of two independent experiments. $^*P < 0.05$ for SOCS2 versus WT mice infected with *T. cruzi*.

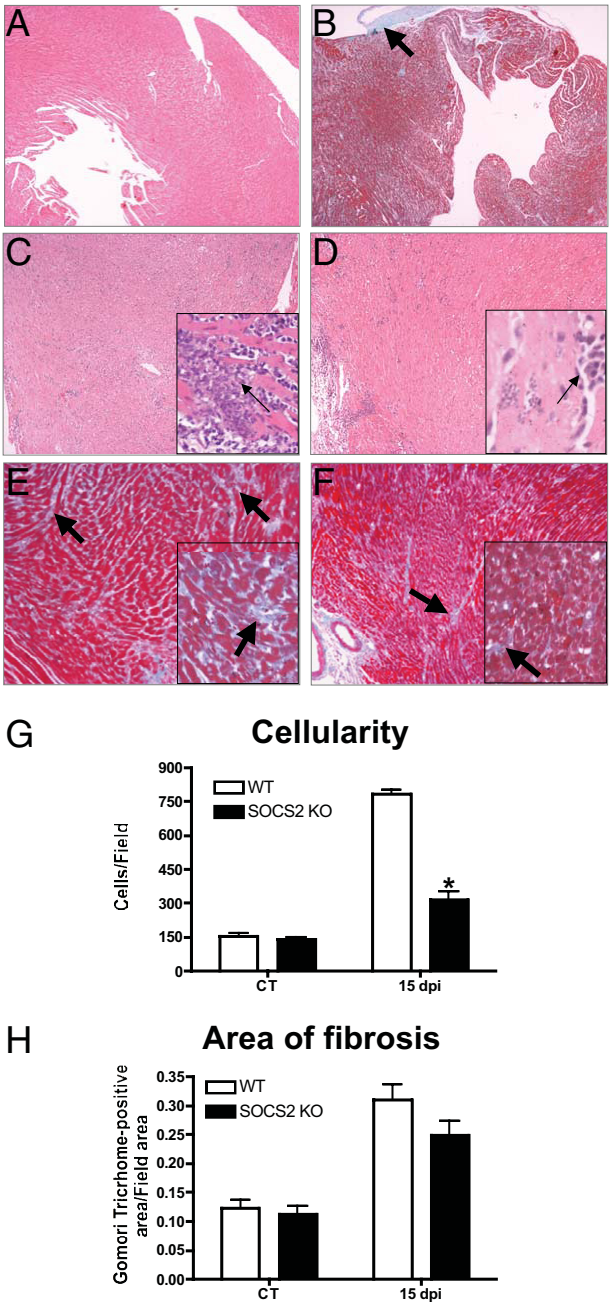

Figure 4. The myocardial pathology was examined in infected WT and SOCS2 KO mice 15 days post infection. Sections of cardiac tissue from WT (**A**,**C**, and **E**) and SOCS2 KO (**B**, **D**, and **F**) mice were either uninfected (**A** and **B**) or infected (**C**–**F**) with 10^3 trypomastigotes, fixed, and then stained with H&E and Gomori's Trichrome. **Thin arrows** indicate tissue inflammatory infiltrate (**C** and **D**), and **thick arrows** indicate the site of fibrosis (**E** and **F**) in the tissue. The inflammatory score **(G)** and the cardiac fibrosis (**H**) are shown. $^*P < 0.001$ for SOCS2 versus WT mice infected with *T. cruzi*. Original magnification: ×4 (**A** and **B**); ×10 (**C** and **D**); ×20 (**E** and **F**); ×40 (**C**–**F insets)**. The myocardial inflammation was reduced in infected SOCS2 KO mice compared to infected WT mice. Data are shown as the means ± SD and are representative of two independent experiments. $^*P < 0.05$ for SOCS2 versus WT mice infected with *T. cruzi*.

development of myocarditis during *T. cruzi* infection prompted the examination of these mice for any evidence of myocardial dysfunction. Echocardiography performed 15 days post infection demonstrated no significant differences in right ventricular area or ejection fraction (Figure 5, A and B) in infected WT or SOCS2 KO mice compared with uninfected mice. Infected SOCS2 KO mice displayed cardiac hypertrophy as determined by higher fraction of circumferential area and increased left ventricular mass when compared with WT animals (Figure 5, C and D).

Patch clamping and confocal microscopy were used to evaluate cardiac myocyte physiology because changes in electrophysiological properties and calcium

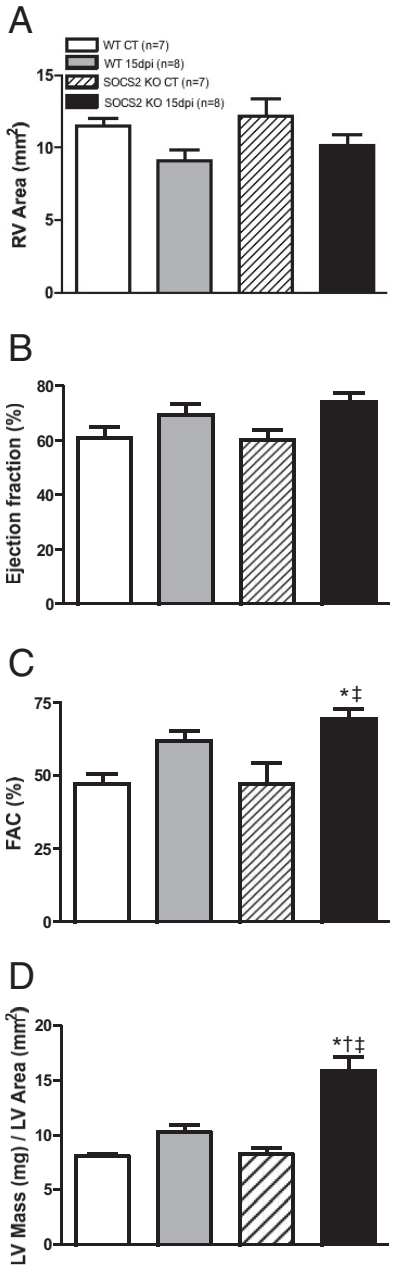

Figure 5. Evaluation of cardiac hypertrophy in infected SOCS2 KO mice. Cardiac function of WT and SOCS2 KO mice infected with 1000 trypomastigotes of *T. cruzi* as assessed by echocardiography. **A:** Right ventricular (RV) area, ejection fraction (EF) (**B**), fraction of circumferential area (FAC) (**C**), and left ventricular hypertrophy computed from LV mass (mg)/LV (**D**) area (mm^2). $^*P < 0.05$ versus WT uninfected, $^\dagger P < 0.05$ versus WT infected, and $^\ddagger P < 0.05$ versus SOCS2 KO uninfected. Infected SOCS2 KO mice displayed cardiac hypertrophy as determined by higher FAC and increased LV mass when compared with WT animals (**C** and **D**). CT, control.

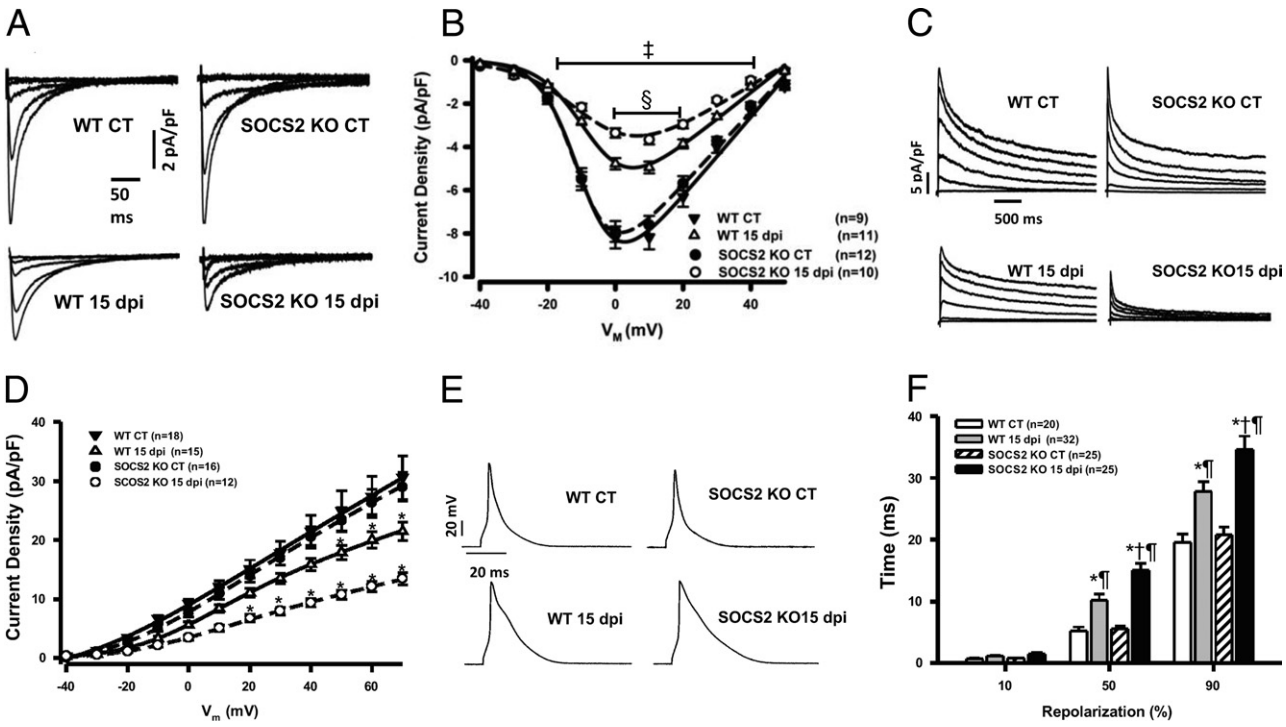

Figure 6. The consequence of the absence of SOCS2 alters the electrophysiological characteristics of cardiac myocytes during *T. cruzi* infection. **A:** Representative L-type calcium current ($I_{Ca,L}$) recordings from WT CT, WT 15 dpi, SOCS2 KO CT, SOCS2 KO 15 dpi. **B:** Voltage dependence of $I_{Ca,L}$, plotted as current density (pA/pF) from −40 to 50 mV for WT CT, WT 15 dpi, SOCS2 KO CT, SOCS2 KO 15 dpi). **C:** Representative transient outward potassium current (I_{to}) recordings from WT CT, WT 15 dpi, SOCS2 KO CT, SOCS2 KO 15 dpi. **D:** Voltage dependence of I_{to}, plotted as current density (pA/pF) from −40 to 70 mV for WT CT, WT 15, SOCS2 KO CT, SOCS2 KO 15 dpi). **E:** Representative action potential (AP) from WT CT, WT 15 dpi, SOCS2 KO CT, SOCS2 KO 15 dpi. **F:** Bar graphs comparing AP repolarization time at different repolarization levels. n = number of cells. **B:** $^{\ddagger}P < 0.05$ SOCS2 KO 15 dpi and WT 15 dpi versus WT and SOCS2 KO uninfected; $^{\S}P < 0.05$ SOCS2 KO 15 dpi versus WT 15 dpi. **D:** $^{*}P < 0.05$ WT 15 dpi and SOCS2 15 dpi versus WT and SOCS2 KO uninfected. **F:** Parameters were significantly increased in SOCS2 infected mice. $^{*}P < 0.05$ versus WT uninfected; $^{\dagger}P < 0.05$ versus WT 15 dpi; and $^{\P}P < 0.05$ versus SOCS2 KO uninfected. CT, control; dpi, days post infection.

handling are a major cause of heart failure.[24,27] Reduced L-type calcium and outward potassium currents in SOCS2 deficient cardiac myocytes were observed 15 days post infection compared to infected WT mice (Figure 6, A–D). However, in uninfected WT and SOCS2 KO mice, L-type calcium and outward potassium currents, and action potential repolarization were almost identical. Furthermore, infected SOCS2 KO mice displayed an increased time to action potential repolarization when compared with WT mice (Figure 6, E and F). Typical line-scan fluorescence images recorded from electrically stimulated Fluo-4 AM–loaded ventricular myocytes are shown in Figure 7, A and B. *T. cruzi* infection led to a significant increase in the amplitude of the calcium transient in cardiac myocytes isolated 15 days after infection (Figure 7) (peak Ca^{2+} F/F_0, WT control: 3.362 ± 0.091, n = 84 isolated cells; WT infected: 3.986 ± 0.133, n = 82 isolated cells; $P < 0.001$). There was no difference in the kinetics of decay of the calcium transient (T50, ms) after infection of cardiac myocytes (Figure 7) (WT control: 266.1 ± 5.879, n = 84 isolated cells; WT infected: 261.4 ± 6.695, n = 82 isolated cells). In SOCS2-deficient cardiac myocytes, there was an increase in calcium transient after infection that was only slightly smaller than in infected WT mice (Figure 7) (peak Ca^{2+} F/F_0, WT infected: 3.986 ± 0.133, n = 82 isolated cells; and SOCS2

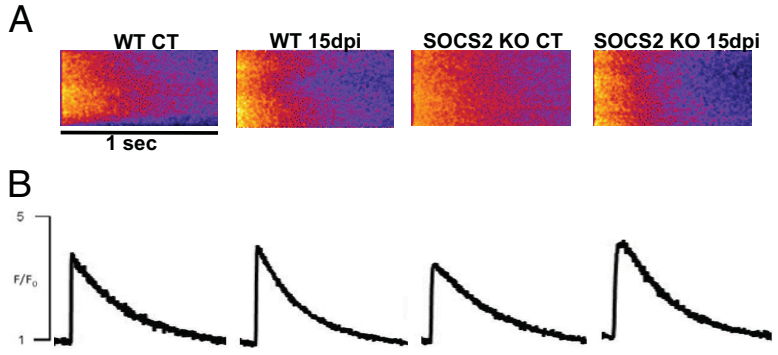

Figure 7. *T. cruzi* infection alters calcium handling in ventricular myocytes from SOCS2 KO mice. The *T. cruzi* infection increased the peak Ca^{2+} transient amplitude in cardiomyocytes obtained from WT and SOCS2 KO mice, but changed the decay kinetics of only the infected SOCS2 KO mice. **A:** Representative confocal images of electrically stimulated intracellular Ca^{2+} transient recordings in ventricular myocytes. **B:** Representative Ca^{2+} transient line-scan profile. CT, uninfected mice; dpi, days post infection.

KO infected: 3.835 ± 0.154, $n = 54$ isolated cells). In addition, the kinetics of decay of the calcium transient after infection of cardiac myocytes was slower in infected SOCS2-deficient cardiac myocytes than infected WT (Figure 7) (WT infected: 261.4 ± 6.695, $n = 82$ isolated cells; and SOCS2 KO infected: 294.9 ± 7.509, $n = 54$ isolated cells; $P < 0.05$).

Discussion

We have described, for the first time, the role of SOCS2 in the pathogenesis of an experimental model of Chagas disease. Our results can be summarized as follows: i) *T. cruzi* infection induced SOCS2 expression in the heart of mice that was, in part, dependent on the activation of the 5-LO pathway; ii) SOCS2 deficiency resulted in reduction in peripheral parasitemia, but not in heart parasitism, and in the down-modulation of proinflammatory cytokines, including TNF-α, IL-12, and IFN-γ, and reduced myocardial inflammation; iii) although IFN-γ was reduced, SOCS2-deficient macrophages were hyperresponsive to this cytokine and dealt with infection more efficiently; iv) mechanistically, enhanced number of Treg cells and enhanced levels of LXA_4 were associated with decreased inflammatory responses and reduced production of proinflammatory mediators; and v) in the absence of SOCS2, there was myocardial (hypertrophy) and cardiac myocyte (altered calcium handling) dysfunction. Altogether, these results clearly show that SOCS2 expression facilitates inflammatory and immune responses in *T. cruzi*–infected mice at the cost of preventing myocardial dysfunction.

Initial experiments demonstrated that SOCS2 expression induced by *T. cruzi* infection was partially dependent on the 5-LO pathway. This pathway has received attention in the field of inflammation research because of the association of infection and leukotriene B (LTB) synthesis. LTBs have been reported to be important in the control of infection by protozoan parasites.[28,29] In addition to LTBs, 5-LO induces LXA_4 production that triggers the AhR receptor altering the expression of SOCS2.[16] These results suggest that production of a 5-LO–derived molecule, presumably LXA_4, contributes to SOCS2 expression during experimental *T. cruzi* infection. It is interesting to notice that the phenotype of 5-LO–deficient mice infected with *T. cruzi*[30] is similar to those observed here. Indeed, absence of 5-LO was associated with decreased inflammatory infiltrate and production of proinflammatory cytokines,[30] suggesting that in addition to absence of LTB, decreased expression of SOCS2 could account for the phenotype observed in 5-LO–deficient mice. Since there was still increased SOCS2 expression in the absence of 5-LO, our results also suggest that other pathways may be involved in SOCS2 expression on infection.

SOCS2 deficiency resulted in a reduction in peripheral parasitemia, but not in heart parasitism, even in presence of reduced expression of IFN-γ. The *in vitro* observations suggest that resistance to infection (parasite replication) could be attributable to an increased ability of SOCS2-deficient macrophages stimulated with IFN-γ to kill intracellular amastigotes via increased production of NO. We found that SOCS2-deficient macrophages were hyperresponsive to IFN-γ stimulation, which could be attributed to reduced inhibition of IFN-γ receptor signaling. Interestingly, *T. cruzi*–infected SOCS2 KO macrophages that are not stimulated with cytokines release greater numbers of trypomastigotes in the culture supernatants compared with WT cells despite producing a similar concentration of NO. Further studies are required to understand the molecular mechanisms underlying these observations.

Absence of SOCS2 was clearly associated with decreased levels of cytokines in spleen and heart of *T. cruzi*–infected mice and decreased inflammatory infiltrate. This was at first a unexpected finding, because SOCS2 is known to suppress the function of cytokines. Hence, absence of SOCS2 would presumably be associated with enhanced cytokine responses. However, two observations help to explain our results. In the absence of SOCS2, there were greater numbers of Treg cells and enhanced production of LXA_4.

The role of Treg in experimental *T. cruzi* infection is still somewhat controversial.[31] Part of this controversy stems from the difficulty in depleting specifically Treg cells *in vivo* and in differences of experimental models used. However, $CD4^+CD25^+$ cells expressing FoxP3 have been shown to associate with better outcome in chagasic patients.[32] Moreover, an increased frequency of Treg cells was found during the acute phase of experimental *T. cruzi* infection in mice.[31] In mice, there is also evidence to show that Treg cells migrate to the heart of infected mice and may have a protective role.[33] Taken together, these studies suggest that Treg cells likely control disease severity during *T. cruzi* infection. Therefore, the enhanced numbers of Treg cells in SOCS2 KO mice may explain the reduced tissue inflammation observed in these mice. Production of anti-inflammatory cytokines, including IL-10 and TGF-β, account for most of the immunosuppressive effects of Treg cells in various experimental systems.[34] In our model, SOCS2 was not associated with increased production of IL-10, but with enhanced expression of TGF-β, suggesting the latter is the major pathway by which Treg cells may alter immune function in SOCS2-deficient mice. It is not clear why absence of SOCS2 would result in greater numbers of Treg cells after *T. cruzi* infection. AhR, a lipoxin receptor that may trigger SOCS2 expression, modifies Treg balance by modifying the cytokine milieu.[35] Therefore, we are currently investigating the possibility of induction of SOCS2 expression by activation of AhR receptor during *T. cruzi* infection as a modulator of Treg generation and expansion.

There was an increase in levels of LXA_4 in SOCS2 KO mice after *T. cruzi* infection. Because LXA_4 is an effective anti-inflammatory molecule,[36,37] enhanced levels of this lipid could account, at least partially, for the reduced inflammation and production of proinflammatory cytokines. It must be noted that LXA_4 may function in SOCS2-dependent and -independent manners. As the lipid was enhanced in the absence of SOCS2, it is clear that SOCS2-independent pathways could be operational in the latter animals to mediate any anti-inflammatory actions of LXA_4.

Severe chronic Chagas heart disease is characterized by dilation of chambers, decreased ejection fraction, and electrical instability.[6] In our system, evaluation of heart function in WT mice at 15 days after infection was not associated with any major changes in heart function. Only when experiments were conducted in SOCS2-deficient mice did we notice that LV mass was increased and the fraction of circumferential area enhanced, suggesting that there were compensatory mechanisms operating at this early stage in these mice to prevent dysfunction. Overall, these data are indicative that SOCS2 deficient mice are more likely to develop heart dysfunction on infection. Electrophysiological studies showed that infection caused reduction of the outward potassium current and in L-type calcium current amplitude. These changes were more marked in the absence of SOCS2 and the calcium transient was also prolonged. Altogether, these changes in SOCS2-deficient mice could lead to greater duration of the action potential that could provide an electrophysiological basis for the echocardiographic findings. It has been demonstrated that different cytokines can modulate ionic currents in isolated cardiac myocytes.[38,39] A correlation between reduced cardiac myocyte shortening and increased levels of TNF-α and IFN-γ during *T. cruzi* infection has been previously demonstrated.[23] It is still unclear how the profile of cytokines found in the absence of SOCS2 correlates with the altered cardiac myocyte electrical remodeling. However, results showing decreased expression of SOCS1 and SOCS3 may provide an explanation to our findings. SOCS1 and SOCS3 expression is known to counteract the actions of molecules, such as IL-6, which induce cardiac myocyte hypertrophy.[40] For example, leukemia inhibitory factor (LIF), a member of the IL-6 family, has been reported to increased $I_{Ca,L}$ thought activation of ERK, a pathway known to be blocked by SOCS.[41] Because there was reduced SOCS1 and SOCS3 in SOCS2-deficient mice, one would expect greater ability of the inflammatory milieu found in the infected heart to induce more hypertrophy. However, the mediators of this hypertrophic response still need to be identified.

In summary, this report demonstrates the importance of SOCS2 in the modulation of experimental *T. cruzi* infection. In the absence of SOCS2, there is decreased inflammation and parasitemia, which are associated with an increase in the number of Treg cells and the LXA_4 levels. This occurs at the cost of greater infection-associated heart dysfunction. Therefore, the expression of SOCS2 during *T. cruzi* infection decreases heart dysfunction at the cost of greater parasitemia and tissue inflammation. These studies highlight the role of SOCS2 in balancing immune and physiological functions in the heart of animals subjected to an infections insult.

References

1. Morris SA, Tanowitz HB, Wittner M, Bilezikian JP: Pathophysiological insights into the cardiomyopathy of Chagas' disease. Circulation 1990, 82:1900–1909
2. Huang H, Calderon TM, Berman JW, Braunstein VL, Weiss LM, Wittner M, Tanowitz HB: Infection of endothelial cells with Trypanosoma cruzi activates NF-kappaB and induces vascular adhesion molecule expression. Infect Immun 1999, 67:5434–5440
3. Mukherjee S, Huang H, Petkova SB, Albanese C, Pestell RG, Braunstein VL, Christ GJ, Wittner M, Lisanti MP, Berman JW, Weiss LM, Tanowitz HB: Trypanosoma cruzi infection activates extracellular signal-regulated kinase in cultured endothelial and smooth muscle cells. Infect Immun 2004, 72:5274–5282
4. Tanowitz HB, Gumprecht JP, Spurr D, Calderon TM, Ventura MC, Raventos-Suarez C, Kellie S, Factor SM, Hatcher VB, Wittner M, Berman J: Cytokine gene expression of endothelial cells infected with Trypanosoma cruzi. J Infect Dis 1992, 166:598–603
5. Tanowitz HB, Kaul DK, Chen B, Morris SA, Factor SM, Weiss LM, Wittner M: Compromised microcirculation in acute murine Trypanosoma cruzi infection. J Parasitol 1996, 82:124–130
6. Marin-Neto JA, Cunha-Neto E, Maciel BC, Simoes MV: Pathogenesis of chronic Chagas heart disease. Circulation 2007, 115:1109–1123
7. Silva JS, Morrissey PJ, Grabstein KH, Mohler KM, Anderson D, Reed SG: Interleukin 10 and interferon gamma regulation of experimental Trypanosoma cruzi infection. J Exp Med 1992, 175:169–174
8. Silva JS, Vespa GN, Cardoso MA, Aliberti JC, Cunha FQ: Tumor necrosis factor alpha mediates resistance to Trypanosoma cruzi infection in mice by inducing nitric oxide production in infected gamma interferon-activated macrophages. Infect Immun 1995, 63:4862–4867
9. Torrico F, Heremans H, Rivera MT, Van Marck E, Billiau A, Carlier Y: Endogenous IFN-gamma is required for resistance to acute Trypanosoma cruzi infection in mice. J Immunol 1991, 146:3626–3632
10. Almeida IC, Gazzinelli RT: Proinflammatory activity of glycosylphosphatidylinositol anchors derived from Trypanosoma cruzi: structural and functional analyses. J Leukoc Biol 2001, 70:467–477
11. Shoda LK, Kegerreis KA, Suarez CE, Roditi I, Corral RS, Bertot GM, Norimine J, Brown WC: DNA from protozoan parasites Babesia bovis. Trypanosoma cruzi, and T brucei is mitogenic for B lymphocytes and stimulates macrophage expression of interleukin-12, tumor necrosis factor alpha, and nitric oxide. Infect Immun 2001, 69:2162–2171
12. Camargo MM, Almeida IC, Pereira ME, Ferguson MA, Travassos LR, Gazzinelli RT: Glycosylphosphatidylinositol-anchored mucin-like glycoproteins isolated from Trypanosoma cruzi trypomastigotes initiate the synthesis of proinflammatory cytokines by macrophages. J Immunol 1997, 158:5890–5901
13. Cardillo F, Voltarelli JC, Reed SG, Silva JS: Regulation of Trypanosoma cruzi infection in mice by gamma interferon and interleukin 10: role of NK cells. Infect Immun 1996, 64:128–134
14. Silva JS, Twardzik DR, Reed SG: Regulation of Trypanosoma cruzi infections in vitro and in vivo by transforming growth factor beta (TGF-beta). J Exp Med 1991, 174:539–545
15. Rico-Bautista E, Flores-Morales A, Fernandez-Perez L: Suppressor of cytokine signaling (SOCS) 2, a protein with multiple functions. Cytokine Growth Factor Rev 2006, 17:431–439
16. Machado FS, Johndrow JE, Esper L, Dias A, Bafica A, Serhan CN, Aliberti J: Anti-inflammatory actions of lipoxin A4 and aspirin-triggered lipoxin are SOCS-2 dependent. Nat Med 2006, 12:330–334
17. Tannahill GM, Elliott J, Barry AC, Hibbert L, Cacalano NA, Johnston JA: SOCS2 can enhance interleukin-2 (IL-2) and IL-3 signaling by accelerating SOCS3 degradation. Mol Cell Biol 2005, 25:9115–9126
18. Knosp CA, Carroll HP, Elliott J, Saunders SP, Nel HJ, Amu S, Pratt JC, Spence S, Doran E, Cooke N, Jackson R, Swift J, Fitzgerald DC, Heaney LG, Fallon PG, Kissenpfennig A, Johnston JA: SOCS2 regulates T helper type 2 differentiation and the generation of type 2 allergic responses. J Exp Med 2011, 208:1523–1531
19. Machado FS, Aliberti J: Impact of lipoxin-mediated regulation on immune response to infectious disease. Immunol Res 2006, 35:209–218
20. Chen XS, Sheller JR, Johnson EN, Funk CD: Role of leukotrienes revealed by targeted disruption of the 5-lipoxygenase gene. Nature 1994, 372:179–182
21. Metcalf D, Greenhalgh CJ, Viney E, Willson TA, Starr R, Nicola NA, Hilton DJ, Alexander WS: Gigantism in mice lacking suppressor of cytokine signalling-2. Nature 2000, 405:1069–1073
22. Machado FS, Martins GA, Aliberti JC, Mestriner FL, Cunha FQ, Silva JS: Trypanosoma cruzi-infected cardiomyocytes produce chemokines and cytokines that trigger potent nitric oxide-dependent trypanocidal activity. Circulation 2000, 102:3003–3008
23. Roman-Campos D, Duarte HL, Sales PA Jr., Natali AJ, Ropert C, Gazzinelli RT, Cruz JS: Changes in cellular contractility and cytokines

profile during Trypanosoma cruzi infection in mice. Basic Res Cardiol 2009, 104:238–246
24. Roman-Campos D, Campos AC, Gioda CR, Campos PP, Medeiros MA, Cruz JS: Cardiac structural changes and electrical remodeling in a thiamine-deficiency model in rats. Life Sci 2009, 84:817–824
25. Lang RM, Bierig M, Devereux RB, Flachskampf FA, Foster E, Pellikka PA, Picard MH, Roman MJ, Seward J, Shanewise J, Solomon S, Spencer KT, St John Sutton M, Stewart W; American Society of Echocardiography' S Nomenclature and Standards Committee; Task Force on Chamber Quantification; American College of Cardiology Echocardiography Committee; American Heart Association; European Association of Echocardiography; European Society of Cardiology: Recommendations for chamber quantification. Eur J Echocardiogr 2006, 7:79–108
26. Guatimosim S, Sobie EA, dos Santos Cruz J, Martin LA, Lederer WJ: Molecular identification of a TTX-sensitive Ca(2+) current. Am J Physiol Cell Physiol 2001, 280:C1327–C1339
27. Gomez AM, Valdivia HH, Cheng H, Lederer MR, Santana LF, Cannell MB, McCune SA, Altschuld RA, Lederer WJ: Defective excitation-contraction coupling in experimental cardiac hypertrophy and heart failure. Science 1997, 276:800–806
28. Henderson WR Jr., Chi EY: The importance of leukotrienes in mast cell-mediated Toxoplasma gondii cytotoxicity. J Infect Dis 1998, 177: 1437–1443
29. Machado ER, Ueta MT, Lourenco EV, Anibal FF, Sorgi CA, Soares EG, Roque-Barreira MC, Medeiros AI, Faccioli LH: Leukotrienes play a role in the control of parasite burden in murine strongyloidiasis. J Immunol 2005, 175:3892–3899
30. Pavanelli WR, Gutierrez FR, Mariano FS, Prado CM, Ferreira BR, Teixeira MM, Canetti C, Rossi MA, Cunha FQ, Silva JS: 5-Lipoxygenase is a key determinant of acute myocardial inflammation and mortality during Trypanosoma cruzi infection. Microbes Infect 2010, 12: 587–597
31. Tonelli RR, Torrecilhas AC, Jacysyn JF, Juliano MA, Colli W, Alves MJ: In vivo infection by Trypanosoma cruzi: the conserved FLY domain of the gp85/trans-sialidase family potentiates host infection. Parasitology 2011, 138:481–492
32. Sathler-Avelar R, Vitelli-Avelar DM, Teixeira-Carvalho A, Martins-Filho OA: Innate immunity and regulatory T-cells in human Chagas disease: what must be understood?. Mem Inst Oswaldo Cruz 2009; 104(Suppl 1):246–251
33. Mariano FS, Gutierrez FR, Pavanelli WR, Milanezi CM, Cavassani KA, Moreira AP, Ferreira BR, Cunha FQ, Cardoso CR, Silva JS: The involvement of CD4+CD25+ T cells in the acute phase of Trypanosoma cruzi infection. Microbes Infect 2008, 10:825–833
34. Josefowicz SZ, Lu LF, Rudensky AY: Regulatory T cells: mechanisms of differentiation and function. Annu Rev Immunol 2012, 30:531–564
35. Stevens EA, Mezrich JD, Bradfield CA: The aryl hydrocarbon receptor: a perspective on potential roles in the immune system. Immunology 2009, 127:299–311
36. Serhan CN: Resolution phase of inflammation: novel endogenous anti-inflammatory and proresolving lipid mediators and pathways. Annu Rev Immunol 2007, 25:101–137
37. Machado FS, Aliberti J: Role of lipoxin in the modulation of immune response during infection. Int Immunopharmacol 2008, 8:1316–1319
38. Fernandez-Velasco M, Ruiz-Hurtado G, Hurtado O, Moro MA, Delgado C: TNF-alpha downregulates transient outward potassium current in rat ventricular myocytes through iNOS overexpression and oxidant species generation. Am J Physiol Heart Circ Physiol 2007, 293:H238–H245
39. Hagiwara Y, Miyoshi S, Fukuda K, Nishiyama N, Ikegami Y, Tanimoto K, Murata M, Takahashi E, Shimoda K, Hirano T, Mitamura H, Ogawa S: SHP2-mediated signaling cascade through gp130 is essential for LIF-dependent I CaL, [Ca2+]i transient, and APD increase in cardiomyocytes. J Mol Cell Cardiol 2007, 43:710–716
40. Takahashi N, Saito Y, Kuwahara K, Harada M, Tanimoto K, Nakagawa Y, Kawakami R, Nakanishi M, Yasuno S, Usami S, Yoshimura A, Nakao K: Hypertrophic responses to cardiotrophin-1 are not mediated by STAT3, but via a MEK5-ERK5 pathway in cultured cardiomyocytes. J Mol Cell Cardiol 2005, 38:185–192
41. Kato T, Sano M, Miyoshi S, Sato T, Hakuno D, Ishida H, Kinoshita-Nakazawa H, Fukuda K, Ogawa S: Calmodulin kinases II and IV and calcineurin are involved in leukemia inhibitory factor-induced cardiac hypertrophy in rats. Circ Res 2000, 87:937–945